DNA Nanotechnology

Deutsche Ausgabe: DOI: 10.1002/ange.201601944
Internationale Ausgabe: DOI: 10.1002/anie.201601944

Self-Assembly of Complex DNA Tessellations by Using Low-Symmetry Multi-arm DNA Tiles

Fei Zhang, Shuoxing Jiang, Wei Li, Ashley Hunt, Yan Liu,* and Hao Yan**

Abstract: *Modular DNA tile-based self-assembly is a versatile way to engineer basic tessellation patterns on the nanometer scale, but it remains challenging to achieve high levels of structural complexity. We introduce a set of general design principles to create intricate DNA tessellations by employing multi-arm DNA motifs with low symmetry. We achieved two novel Archimedean tiling patterns, (4.8.8) and (3.6.3.6), and one pattern with higher-order structures beyond the complexity observed in Archimedean tiling. Our success in assembling complicated DNA tessellations demonstrates the broad design space of DNA structural motifs, enriching the toolbox of DNA tile-based self-assembly and expanding the complexity boundaries of DNA tile-based tessellation.*

The fabrication of two-dimensional (2D) nanostructures with designed patterns has attracted broad interest because these structures provide unique physical and chemical properties that differ from those of their bulk phases.[1] In contrast to regular tessellation arrangements, Archimedean tilings and quasicrystalline structures possess geometric complexity that can lead to unusual catalytic,[2] electronic,[3] or optical[4] properties. Structural DNA nanotechnology offers unparalleled programmability for engineering nanoscale patterns with an extraordinarily high level of structural control[5] and has already proven useful in designing and engineering intricate 2D patterns such as Archimedean tilings.[6] In this work, we introduce a general design strategy to create multi-arm DNA junctions with reduced symmetry and proper matching rules to satisfy the critical requirements for creating complex tessellation patterns. This strategy enabled the successful construction of two novel DNA Archimedean tilings, (4.8.8) and (3.6.3.6), as well as an intricate pattern with higher-order structures beyond the complexity observed in Archimedean tilings, thus demonstrating the unique programmability of DNA nanotechnology for complex pattern formation.

To create (4.8.8) and (3.6.3.6) Archimedean tiling patterns, we first needed to design 3- and 4-arm DNA tile motifs with lower geometric symmetry (2-fold instead of 3- or 4-fold). These tile motifs are based on symmetric 3×4 and 4×4 tiles that have bending and flexibility between neighboring arms.[7] Our previous work has shown that 3T (3 thymine nucleotides) loops can be used to form both 3- and 4-arm motifs,[8] thus indicating that the 3T loops connecting the neighboring arms have a range of flexibility that allows the formation of a relatively wide range of angles spanning 80 to 135°. DNA motifs with different symmetry are achieved either by introducing a specific matching rule that is encoded by the sequences of the sticky ends (Figure 1 A, C) or in combination with different loop lengths (Figure 1 B, D). As shown in Figure 1 A, we converted a 3-arm motif with 3-fold symmetry into a new 3-arm motif with 2-fold symmetry by assigning inter-arm angles of 90, 135, and 135°. The sticky ends are then designed to first connect the 3-arm motif into a square unit cell with four outward protruding sticky ends that further self-assemble into the (4.8.8) Archimedean tiling referred to as "truncated square tiling" (Figure 1 C). We also reduced the symmetry of the 4-arm motif to exhibit 2-fold symmetry with inter-arm angles of 120 and 60°. The sticky-end design then allows connection of three of these building

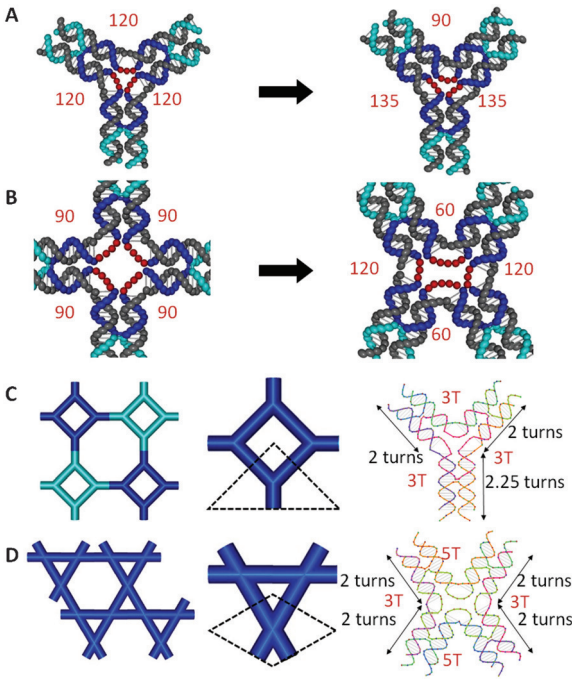

Figure 1. An illustration of the design of multi-arm DNA junction motifs with reduced symmetry. A, B) Schematics of 3- and 4-arm motifs with different branch angles tuned by the lengths of the single-stranded poly-T loops on the central strand. C, D) The patterns (left) and their units (center) of the two Archimedean tilings. (C) shows the truncated square tiling noted as (4.8.8), and (D) shows the trihexagonal tiling (also called a Kagome lattice) referred to as (3.6.3.6). The corresponding DNA tile designs are shown on the right.

[*] Dr. F. Zhang, S. Jiang, Dr. W. Li, A. Hunt, Prof. Y. Liu, Prof. H. Yan
School of Molecular Sciences and The Biodesign Institute
Arizona State University, Tempe, AZ 85287 (USA)
E-mail: fei.zhang@asu.edu
yan_liu@asu.edu
hao.yan@asu.edu

Supporting information for this article can be found under: http://dx.doi.org/10.1002/anie.201601944.

blocks to form a triangular unit cell (Figure 1D) that will further self-assemble into 2D patterns called trihexagonal tiling (3.6.3.6), also known as the Kagome lattice.

We propose several design principles that should be used to implement complex DNA tessellations based on these asymmetric motifs. First, the lengths of the central single-stranded loops at each vertex should be adjusted to accommodate the desired angles and distance between branches (e.g., Figure 1D). Second, the types and numbers of DNA motifs in each of the unit cells should be carefully selected such that specific recognitions between tiles allows just one desired repeating unit. Third, the edge length of each tessellation pattern is restricted to even (non-corrugated design) or odd (corrugated design) numbers of half-turns. This ensures minimal structural twisting and strain in the final assembly in a 2D array, considering that B-form double-stranded DNA is a 3D molecule with 10.5 base pairs (bp) per helical turn in solution. Fourth, the appropriate matching rules should be designed to guide interactions between repeating units to avoid any spurious interactions. Finally, external experimental conditions, such as hierarchical stepwise annealing and surface-mediated growth, can be applied to facilitate the formation of complex patterns or to flatten structures.

By following these principles, we initially tested four design options for the truncated square tiling (Figure S1 in the Supporting Information). The unit cell of this pattern contains four 3-arm tiles connected to form a square with four external arms pointing away diagonally. We assigned four distinct 3-arm tiles with matching sticky ends that grow into the unit cell (Figure S1). One of the simplest designs is shown in Figure S1A, in which the four 3-arm tiles all face the same direction (non-corrugated), with their external sticky ends binding the opposite ones without any in-plane rotations or out-of-plane flips. This design only produced partially formed structures. The other three designs are all corrugated[9] with different matching rules: one contains corrugation among the four tiles within the unit but not between the units, one contains corrugation within the unit and in-plane rotation, and one contains no corrugation within the unit but corrugation between neighboring units. The last design successfully produced the correct truncated square 2D tiling with sizes up to several microns (Figure 2A and Figure S1D). The non-corrugated design was not successful (Figure S1A), possibly owing to overly excessive geometry constraints in the individual tiles (e.g., for bending and twisting). Among the three corrugated designs, two yielded small linear arrays (Figure S1B,C), thus indicating undesired helical twist along that direction that prevents the formation of a stable 2D array.

The number of tiles used to construct a unit cell is a critical factor. We attempted to minimize the number of different DNA building blocks required to form the unit cell by considering the geometric symmetry of the unit cells (4- or 2-fold rotational symmetry). However, such symmetry will increase the likelihood of forming undesirable unit cells (e.g., closed structures with numbers of building blocks other than 4) due to a decrease in tile specificity and intrinsic flexibility. For example, when a single 3-arm tile with two complementary (2 and 2*) and one self-complementary (1 = 1*) sticky ends was used to form the square unit cell, atomic force microscopy (AFM) images show that the dominating products are thin tubes with ca. 30 nm diameters (Figure 2B). Although this product is structurally constrained, the matching rules still allow it to form. Therefore, a balance between DNA tile-sequence design simplicity and matching-rule specificity is required to form a unique pattern.

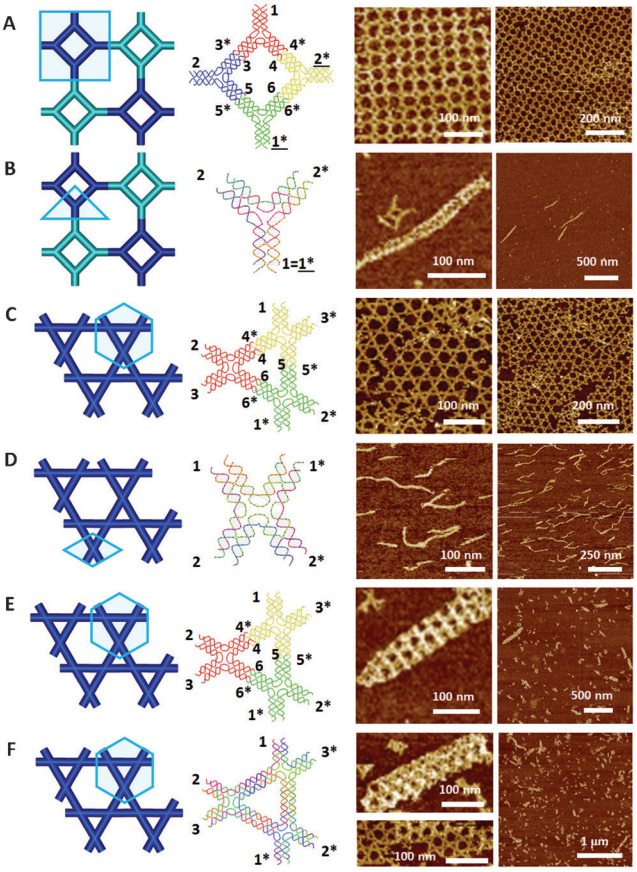

Figure 2. Sticky-end matching rules and corresponding AFM images for the Archimedean tiling designs. A) Truncated square tiling with a four-unique-tile design and the one-pot annealing results. B) Truncated square tiling with a one-tile design and the one-pot annealing results. C) Kagome lattice with a three-unique-tile design and the surface-mediated annealing results. D) Kagome lattice with a one-tile design and the one-pot annealing results. E) Kagome lattice with a three-tile design and the one-pot annealing products. F) Kagome lattice with a sealed-nick design and the one-pot annealing products.

The design that led to large 2D arrays (Figure 2A) often exhibited curved edges on the 2D arrays, thus indicating some curvature out of the 2D plane remaining in the lattice despite careful design of the corrugations among the square units, and we frequently observed wide tubes with diameters of 300–600 nm and partially folded single layers (see additional images in Figure S2 B,C). Tube formation from 2D DNA tile arrays has been discussed previously,[10] It is mainly driven by minimization of system free energy through association of the edge tiles to hide the free dangling sticky ends, and it takes place as long as the enthalpy gain overcomes the entropy loss and enthalpy penalty induced by structure bending and

curving. It is expected that folding of a single layer should take place along the directions with minimal bending energies. We examined the parameters that influence the conformations of the final structures. Based on our truncated square tiling design, there are several possible directions to fold the 2D array, and the folding angle ranges from 45° to 0° (see the schematics and direction defined in Figure S2 A). We carefully examined AFM images of 57 folding edges and found that the majority (35) of edges were folded along the 45° line, (i.e., with the folding edge parallel to the side of the square unit in that pattern), while none of them adopted a folding angle of 0° (i.e., with the edges along the diagonal direction of the square unit; Figure S2 B–D). The preferred folding direction is in accordance with our expectation that the enthalpy gain of sticky-end hybridization should be maximized and the energetic cost of bending should be minimized. For folding along the diagonal direction, two edge sticky ends are paired per length of a unit cell, while for folding along the other direction, only one edge sticky end is paired per length of a unit cell. In addition, junction flexibility accommodates out-of-plane bending in the folding of single layers.

As discussed above, the probability of forming a unique structure is reduced for the unit with the symmetric tile design through the identical repetition one 3-arm motif four times (e.g., the design shown in Figure 2 B). However, when the annealing program was modified to include thermal cycling in the temperature range of 25–40 °C, small incomplete fragments were observed instead of thin tubes (Figure S3). This indicates that instead of a thermodynamic product with minimized free energy, the thin tube is a kinetically trapped product produced during fast nucleation and tube closure (Figure S3).

By following the same design principles used for the truncated square tiling, we next created a Kagome lattice by using three 4-arm DNA motifs (Figure 2 C). To accommodate the desired angles (60, 120, 60, and 120°) for each 4-arm DNA motif, we changed the loops at the vertex from 4T in all cases to alternating 5T, 3T, 5T, 3T between the adjacent branches (Figure 1 B). Three of these 4-arm motifs were connected through matching sticky ends to form a triangular unit cell with six protruding arms that each terminates with double sticky ends (Figure 2 C). The triangular unit cells can further connect to form a Kagome lattice containing alternating small triangles and large hexagons. Corrugation is naturally forbidden in this design.[11] With the desired matching rules shown in Figure 2 C, both surface-mediated folding and one-pot annealing were employed to assemble the samples, and either 2D arrays with frequent facet errors (Figure 2 C) or tubes (Figure 2 E and Figure S4) were produced (for experimental details, see the Supporting Information).

Through a surface-mediated assembly process (Figure 2 C), adhesion of the tile motifs with the mica surface forces the tiles into a 2D plane and thus facilitates the formation of larger arrays. These 2D arrays were still not as large as those seen in the truncated square lattice (Figure 2 A), possibly because the structural strains intrinsic in the tile array cannot be fully accommodated even when a surface is used to help to flatten the tiles. Owing to limited diffusion of the tiles on the mica surface, facet-mismatch errors predominate. Adhesion to the surface may also cause other changes that affect the geometry of the structural units, such as junction flattening, helix stretching, and helical twist.

The one-tile designs with self-complementary sticky ends yielded thin tubes, as for the truncated-square tiling assembly (Figure 2 D in comparison to Figure 2 B). We suspected that the limited growth of the 2D arrays might be due to stoichiometry errors in the strands, so we tried to seal some of the nicks between the sticky ends inside the triangular unit to reduce the total number of strands (Figure 2 F and Figure S5). This step could help minimize potential stoichiometry errors that cause the formation of incomplete structure motifs and thus promote further array growth. The one-pot annealing process produced tubes with the same pattern and similar sizes to those in the original design (Figure 2 F in comparison to Figure 2 E). This result supports the hypothesis that tube formation is due to intrinsic curvature of the structural motifs, which accumulates within the assembly because corrugation is not allowed in the design.

Following the successful construction of the two Archimedean tilings by using asymmetric motifs, we further tested whether our design principles are general enough to produce more intricate patterns with higher-order structures beyond the complexity observed in Archimedean tilings. A more complicated tessellation was designed with two types of asymmetric building blocks: a square unit consisting of four 3-arm motifs and a 4-arm (cross-shaped) tile with two different arm lengths (framed with a blue square and red rectangle, respectively, in Figure 3 A). Besides the design principles described above, an additional problem we encountered was estimating the size of the junction so that the dimensions of the two basic structural units match each other. That is, the total length of the two longer arms of the 4-arm motif plus the size of the center junction should equal the distance between the two outward-protruding sticky ends of the square unit. Different sizes of DNA branches were tested, and the most suitable set is shown in Figure 3 B. Notably, the two units without matching geometries would rather self-sort in the self-assembly process without further growth (Figure S7), which is similar to a previously reported phenomenon.[12] We employed a corrugated design, and the matching rules were assigned accordingly (Figure 3 B). Not surprisingly, the classic one-pot annealing procedure produced fairly well-formed 2D arrays with a size of hundreds of nanometers (Figure 3 C). Considering how complex this system is, with 5 distinct asymmetric motifs and 16 orthogonal sticky-end interactions, the chance of spurious tile interactions is high. We therefore introduced a hierarchical step-wise folding strategy to simplify the self-assembly process in each step and reduce possible mismatches. The two units were annealed separately and then mixed under isothermal conditions (25 °C; for details of the hierarchical folding method, see the Supporting Information). Linear products of each unit were produced in the first annealing step (Figure 3 D), and large 2D lattices up to several microns were obtained in the final mixed samples (Figure 3 E and Figure S8).

In summary, we developed a set of general design principles to create complex DNA tessellations, including

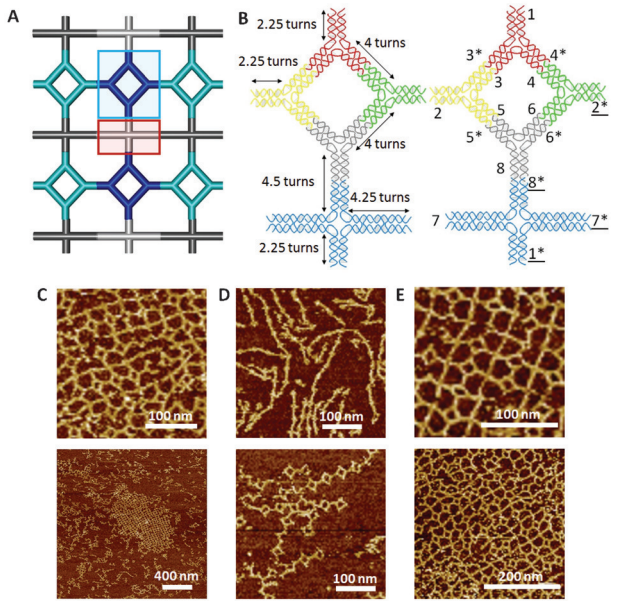

Figure 3. Design and AFM images for the complex DNA tessellation. A) Schematic of the pattern and its two units (in blue and red boxes). B) Optimized arm length (left) and matching rules (right) for the specific motifs. C) AFM images of the one-pot annealing product. D) The first step of hierarchical folding strategy; AFM images show the results of two separately annealed units: the cross-shaped tile and square unit containing four 3-arm motifs. Both form linear arrays. E) The second step of hierarchical folding strategy; AFM images show the formation of 2D arrays after mixing of the two annealed units under isothermal conditions (25 °C).

the two new Archimedean tilings (4.8.8) and (3.6.3.6) and an intricate pattern with higher-order structures beyond the complexity observed in Archimedean tilings. Our strategy has the unique advantage that it can create tessellations composed of diverse polygons with large differences in edge numbers. For example, if we used the previous tile-based assembly method, creating the (4.8.8) pattern would require co-assembly of a 4-arm motif and an 8-arm motif, which would be difficult owing to the dramatic differences in the designs and molecular weights. By using four equal-sized 3-arm motifs that assemble into a square unit, we can easily generate the complicated (4.8.8) pattern. The complex tessellation structures constructed in this work demonstrate the potential power of modular DNA self-assembly to enrich the DNA tile-based assembly toolbox. This work could also enhance the understanding of general DNA self-assembly systems. In the future, our approach for creating sophisticated DNA tessellations could allow the engineering of molecular systems to adopt increasingly complex structures such as quasicrystalline and hyperuniform structures.

Acknowledgements

This research was partly supported by grants to H.Y. and Y.L. from the National Science Foundation (nos. 1360635 and 1334109), the Army Research Office (no. W911NF-12-1-0420), and the National Institutes of Health (no. R01GM104960). H.Y. was supported by the Presidential Strategic Initiative Fund from Arizona State University. The authors thank M. Madjidi for proofreading.

Keywords: Archimedean tiling · DNA nanotechnology · DNA structures · nanostructures · self-assembly

How to cite: *Angew. Chem. Int. Ed.* **2016**, *55*, 8860–8863
Angew. Chem. **2016**, *128*, 9006–9009

[1] J. V. Barth, G. Costantini, K. Kern, *Nature* **2005**, *437*, 671–679.
[2] A. P. Tsai, M. Yoshimura, *Appl. Catal. A* **2001**, *214*, 237–241.
[3] J. Dolinšek, *Chem. Soc. Rev.* **2012**, *41*, 6730–6744.
[4] M. E. Zoorob, M. D. B. Charlton, G. J. Parker, J. J. Baumberg, M. C. Netti, *Nature* **2000**, *404*, 740–743.
[5] a) F. A. Aldaye, A. L. Palmer, H. F. Sleiman, *Science* **2008**, *321*, 1795–1799; b) H. Li, J. D. Carter, T. H. LaBean, *Mater. Today* **2009**, *12*, 24–32; c) A. V. Pinheiro, D. Han, W. M. Shih, H. Yan, *Nat. Nanotechnol.* **2011**, *6*, 763–772; d) N. C. Seeman, *Annu. Rev. Biochem.* **2010**, *79*, 65–87; e) R. F. Service, *Science* **2011**, *332*, 1140–1142; f) R. M. Zadegan, M. L. Norton, *Int. J. Mol. Sci.* **2012**, *13*, 7149–7162; g) F. Zhang, J. Nangreave, Y. Liu, H. Yan, *J. Am. Chem. Soc.* **2014**, *136*, 11198–11211; h) M. Mandelkern, J. G. Elias, D. Eden, D. M. Crothers, *J. Mol. Biol.* **1981**, *152*, 153–161; i) N. C. Seeman, *J. Theor. Biol.* **1982**, *99*, 237–247; j) N. C. Seeman, N. R. Kallenbach, *Biophys. J.* **1982**, *37*, A93–A93.
[6] F. Zhang, Y. Liu, H. Yan, *J. Am. Chem. Soc.* **2013**, *135*, 7458–7461.
[7] C. Zhang, W. Wu, X. Li, C. Tian, H. Qian, G. Wang, W. Jiang, C. Mao, *Angew. Chem. Int. Ed.* **2012**, *51*, 7999–8002; *Angew. Chem.* **2012**, *124*, 8123–8126.
[8] F. Zhang, S. Jiang, S. Wu, Y. Li, C. Mao, Y. Liu, H. Yan, *Nat. Nanotechnol.* **2015**, *10*, 779–784.
[9] a) H. Yan, S. H. Park, G. Finkelstein, J. H. Reif, T. H. LaBean, *Science* **2003**, *301*, 1882–1884; b) W. Liu, H. Zhong, R. Wang, N. C. Seeman, *Angew. Chem. Int. Ed.* **2011**, *50*, 264–267; *Angew. Chem.* **2011**, *123*, 278–281; c) J. Malo, J. C. Mitchell, C. Venien-Bryan, J. R. Harris, H. Wille, D. J. Sherratt, A. J. Turberfield, *Angew. Chem. Int. Ed.* **2005**, *44*, 3057–3061; *Angew. Chem.* **2005**, *117*, 3117–3121.
[10] a) J. C. Mitchell, J. R. Harris, J. Malo, J. Bath, A. J. Turberfield, *J. Am. Chem. Soc.* **2004**, *126*, 16342–16343; b) Y. G. Ke, Y. Liu, J. P. Zhang, H. Yan, *J. Am. Chem. Soc.* **2006**, *128*, 4414–4421.
[11] Y. He, Y. Tian, A. E. Ribbe, C. Mao, *J. Am. Chem. Soc.* **2006**, *128*, 15978–15979.
[12] Y. He, Y. Tian, Y. Chen, A. E. Ribbe, C. Mao, *Chem. Commun.* **2007**, 165–167.

Received: February 24, 2016
Revised: April 28, 2016
Published online: June 8, 2016

